37th European Rotorcraft Forum

Paper n. 125

SIMULATION OF HELICOPTER DYNAMICS WITH EXTERNAL SUSPENDED LOADS

Paolo Marguerettaz

Giorgio Guglieri

Politecnico di Torino - Dipartimento di Ingegneria Aeronautica e Spaziale

Corso Duca degli Abruzzi 24, 10129, Torino, Italy

paolo.marguerettaz@polito.it; giorgio.guglieri@polito.it

ABSTRACT

The present work outlines a short review of available references and technical papers on the flight dynamics of a helicopter carrying a suspended load. A simplified but comprehensive model for helicopter and external suspended load, based on the linear superposition of effects, is defined. This model is then used to evaluate the impact of helicopter configuration (articulated rotors with different state-space representations) and slung load model (pendulum or 6-DOFs suspended body, both spherical and streamlined) on overall system dynamic stability. Impact of load parameters (drag area, mass, length and elastic properties of the suspension line) on the stability of helicopter modal response is also evaluated. Finally the effect of helicopter attitude/rate and suspended load force feedback on the stabilization of the in-flight release phase of the payload is verified.

NOTATION

a	Acceleration
A	Cable cross section
C_D	Drag coefficient
C_L	Lift coefficient
C_M	Pitching moment coefficient
C_N	Yawing moment coefficient
C_S	Sideforce coefficient
D	Drag forces vector
E	Young modulus of the cable
f	Residual
F	Force vector
g	Gravity acceleration
i, j, k	Unit vectors along x, y, z axes
J_x, J_y, J_z, J_{xz}	Moments of inertia
K_G	Gravity forces vector
l	Load length
L	Nominal cable length
M, N	Moments w.r.t. y,z axes
m	Mass
p, q, r	Angular speed w.r.t. x,y,z axes
r	Radius
R	Position vector
S	Reference area
u, v, w	Velocity components along x, y, z axes
V	Velocity vector
X, Y, Z	Forces along x, y, z axes
$[A]$	State space helicopter matrix
$[L_{BE}]$	Rotation matrix from body to inertial axes
$[X]$	States vector
ΔL	Elongation vector (cable)
α	Angle of attack
β	Angle of sideslip
δ	Command input
Ω	Angular velocities vector
φ, θ, ψ	Euler angles
ρ	Air density
ζ	Damping ratio

Superscripts and Subscripts

$\dot{}$	First derivative
$\ddot{}$	Second derivative
$[\ ]^T$	Transposed vector/matrix operator
$[\ ]^{-1}$	Inverse matrix operator
$_A$	Aerodynamic
$_B$	Body frame
$_C$	Cable
$_{crit}$	Critical
$_{CG}$	Centre of mass
$_E$	Ground fixed inertial frame
$_{el}$	Elastic
$_{eff}$	Effective
$_F$	Fuselage
$_H$	Helicopter
$_L$	Load
$_{LS}$	Suspension point (load)
$_{ref}$	Reference
$_{x, y, z}$	x, y, z axes
$_\zeta$	Damping

INTRODUCTION

Carrying external suspended loads is a typical helicopter mission. Both military and commercial operators widely exploits the capabilities of helicopters to rapidly move heavy and bulky loads in impervious locations. Logging, construction, fire fighting, search and rescue, tactical transportation are only some of the possible missions in which a helicopter carries a suspended load. Unfortunately, suspend load adds its aerodynamics, rigid body dynamics and elastic suspension dynamics to that of the bare airframe helicopter. Less than satisfactory handling can result from the combined systems and flight envelope can be significantly degraded with great concern on safety of operations. In fact external suspended load operations account for more than 10% of helicopter accidents, often with severe consequences [1]. A careful study of helicopter dynamics and the assessment of flight and handling qualities is therefore vital for safe operations.

Helicopter dynamics with external suspended load has been widely investigated since the extensive helicopter use in the Vietnam war in the ’60s and ’70s. Early studies focused mainly on hover or low speed flight dealing with reduced order helicopter models, modelling the slung load as a pendulum and neglecting aerodynamics effects [2]. Results showed a stable pendulum mode, but, in some combination of load weight and cable length, helicopter instability could arise. Further works investigated the precision hover with slung load and verified that conventional stability augmentation systems were not up to the task, thus different possible stabilization techniques were studied. Better results were obtained by feeding back to the cyclic the relative motion of load and helicopter [3]. A theoretically good alternative stabilisation scheme required the active displacement of the suspension point, but practical implementation was not explored [4]. Beside electronic stabilisation, appropriate piloting techniques were, also, investigated for various manoeuvres [5]. More recent studies address stability with more complex models. Ref. [6] develops a stability analysis based on a state space helicopter model decoupled in longitudinal and lateral-directional planes. The load is modelled as a pendulum affected by isotropic drag and suspended by an inelastic cable. Results showed stability dependency on both cable length and load weight with the possibility of mildly unstable modes at the increasing of weight and cable length. In Ref. [7] full nonlinear rigid body equations for helicopter dynamics and rotor flap dynamics were derived and then linearised for stability study. Cable length, position of the suspension point with respect to the helicopter centre of mass and load weight all affected stability. Depending on the combination of parameters some modes could experience weak instability.

Most of the previously described studies neglected the aerodynamics of the load because they were focused on hover or low speed flight. Slung loads usually are bluff bodies and may experience instability due to unsteady flows. Studies conducted on containers and cylindrically shaped loads in forward flight showed that increasing cable length, load weight and speed improved stability [8]. These results were only partially confirmed by other works which pointed out that longer cables were destabilizing, but discrepancies can be an effect of the different aerodynamics of the load [9]. Despite most works try to address specific cases, it is generally possible to say that high drag proves to be destabilizing and lateral-directional motions are more affected by load dynamics than longitudinal ones. This is confirmed in Ref. [10] where extensive flight test and frequency response obtained by system identification show that increasing load weight reduces lateral bandwidth, while the longitudinal one is less affected. Ref. [11] analyses helicopter dynamics with suspended load in forward and turning flight. The proposed helicopter model is fully non linear, includes single blades flapping/lagging and rotor inflow and has been validated with flight test data [12]. The load is modelled as a pendulum affected by isotropic drag and suspended by an inelastic cable. Results show that pendulum modes can easily couple with helicopter Dutch roll leading to a degradation of flying qualities while effects on longitudinal motions are much less relevant. Unsteady aerodynamic behaviour of specific loads, in particular containers, has been widely investigated with simulation, wind tunnel testing and flight test [13][14]. It is known that external load instability can reduce safe flight envelope well below limits due to power loading. Ref. [15] provides means to passively stabilise a container, effectively restoring useful flight envelope up to power limits.

Many studies focused on external load modelling. In particular Ref. [16] describes in detail a formulation valid for arbitrary number of loads, suspensions lines and even helicopters. Ref. [17] proposes an interesting formulation to describe a generic slung load system taking into account different suspensions combination and cable collapse and tightening.

Helicopter handling qualities are widely addressed in Ref. [18]. Ref. [19] proposes qualitative and quantitative handling qualities criteria that specifically apply to suspended load operations. In particular, degraded visual environment operations with loads up to 1/3 of the helicopter mass are investigated, because, due to experience, they are considered the most demanding conditions. The quantitative criterion prescribes a lower limit in the available longitudinal and lateral-directional bandwidths. If the bandwidth is superior to the limit, and the helicopter without external load has Level 1 rating on the Cooper Harper scale in the performed manoeuvre, Level 1 rating is assured also with the external load. Below the bandwidth limit, Level 2 rating is still possible if the original helicopter has Level 1 rating. The authors recognise that it is not possible to ascribe a Level 3 rating due to the effects of the external load alone.

PRESENT WORK

First objective of this work is the definition of a simplified but comprehensive model for helicopter and external suspended load based on the linear superposition of effects. This model is then used to evaluate the impact of helicopter configuration (articulated rotors with different state-space representations) and slung load model (pendulum or 6-DOFs suspended body) on overall system dynamic stability. Impact of load parameters (drag area, mass and length of the suspension line) on the stability of helicopter modal response is also evaluated. Finally the effect of helicopter attitude/rate and suspended load force feedback on the stabilization of the in-flight release phase of the payload (drop test) is verified.

MATHEMATICAL MODEL

Reduced order models can be used to obtain a comprehensive approximation of short term longitudinal, lateral directional and heave dynamics when the complete system is weakly coupled as shown in Ref. [20] in the case of articulated rotors. Results presented in Ref. [20] were non in themselves restricted to a small interval of time showing that it is also possible to perform a limited time domain simulation. In any case, when the reduced order model is derived from a higher order representation, it always assumes that the transformation is obtained performing a successful partitioning of states. The dynamic system composed by helicopter and external suspended load can be considered as weakly coupled. As a matter of fact Ref. [11], demonstrates that higher order dynamics, such as rotor and inflow dynamics, has a modest effect on the stability of the lowest frequency modes of the aircraft and the load (frequency and damping of the phugoid, Dutch roll, and load modes do not change by more than about 5 % when rotor and inflow dynamics are taken into account). Hence a quasi-steady rotor model (i.e. incorporating the fuselage states and the suspended load dynamic model) is probably sufficiently accurate to represent the modal response of the vehicle-load system. Furthermore, this approach may balance the level of modelling complexity for the helicopter and the slung load.

Helicopter model

Two articulated rotor tactical utility helicopters are considered, a medium tactical utility and an heavy lift helicopter. The first model derives from the linearization of the non linear model used in Ref. [11]. Data for the second one are from Ref. [21], which is a database of state space matrices and transfer functions obtained by parametric identification of flight test data. Main helicopter characteristics are reported in Tab. 1.

	Helicopter 1	Helicopter 2
Weight [kg]	6800	15800
Rotor radius [m]	8.2	11
Rotor speed [rad/s]	27	19
Blades number	4	6

Tab. 1 – Helicopters main characteristics

In this study the helicopter is modelled as state space model with nine states. State space matrices are obtained in trimmed conditions for different load and forward flight speed. In the solution process helicopter state space matrix coefficients are used to reconstruct the nine equations of motion, evaluating linear and angular velocities and attitude angles in body axes. The state vector is:

$$\left[X_H\right] = \left[u_H, v_H, w_H, p_H, q_H, r_H, \phi_H, \theta_H, \psi_H\right]^T \tag{1}$$

The system is defined as:

$$\left[\dot{X}_H\right] = [A]\left[X_H\right] \tag{2}$$

Where $\dot{X}_H$ is the derived states vector and A the state space matrix.

Three additional equations account for helicopter centre of mass position in an inertial frame. These are, in matrix form:

$$\left[V_{HE}\right] = \left[\dot{x}_{HE}, \dot{y}_{HE}, \dot{z}_{HE}\right]^T = \left[L_{BE_H}\right]\left[u_{HB}, v_{HB}, w_{HB}\right]^T \tag{3}$$

where L_{BE} is the rotation matrix from body axes to a ground fixed frame.

External load as a pendulum

Two approaches have been used to model the external load. In both cases one suspension line only is connected to one point on the helicopter and one on the load. In the first case the load is modelled as a spherical pendulum with the mass supposed concentrated in the centre of mass and suspended from a single point. The only aerodynamic force acting on the pendulum is an isotropic drag. The suspension line is modelled as inextensible, weightless and does not contribute to drag [11].

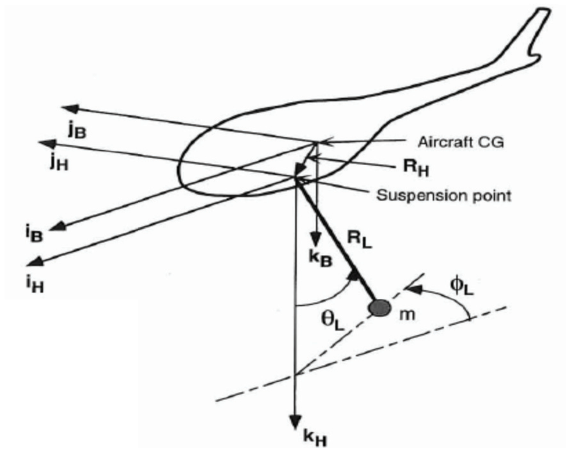

Fig. 1 – System geometry

System geometry is given in Fig. 1. Load position is described by φ_L, the azimuth angle, and by θ_L, the angle between the cable and the z axis. Position vector $\vec{R}_L$ with respect to suspension point is defined as:

$$\vec{R}_L = -L\sin\theta_L \cos\varphi_L \vec{i}_H + L\sin\theta_L \sin\varphi_L \vec{j}_H + L\sin\theta_L \vec{k}_H \quad (4)$$

The position of the suspension point $\vec{R}_H$ with respect to the centre of gravity of the helicopter is:

$$\vec{R}_H = x_H \vec{i}_H + y_H \vec{j}_H + z_H \vec{k}_H \quad (5)$$

The absolute velocity $\vec{V}_L$ of the load is:

$$\vec{V}_L = \vec{V}_{CG} + \dot{R} + \vec{\Omega} \times \vec{R} \quad (6)$$

where $\vec{R} = \vec{R}_H + \vec{R}_L$ is the position vector of the load with respect to the centre of mass of the helicopter and $\vec{\Omega} = p\vec{i}_B + q\vec{j}_B + r\vec{k}_B$ is its angular velocity. The absolute acceleration of the load is:

$$\vec{a}_L = \vec{a}_{CG} + \ddot{R} + \dot{\vec{\Omega}} \times \vec{R} + 2\vec{\Omega} \times \dot{R} + \vec{\Omega} \times \left(\vec{\Omega} \times \vec{R}\right) \quad (7)$$

where $\vec{a}_{CG}$ is the acceleration of the centre of mass of the helicopter. The weight vector is defined as:

$$\vec{F}_G = mg\left(-\sin\varphi_F \vec{i}_H + \sin\varphi_F \cos\theta_F \vec{j}_H + \cos\varphi_F \cos\varphi_F \vec{k}_H\right) \quad (8)$$

where φ_F and θ_F are the roll and pitch attitudes of the helicopter fuselage. The aerodynamic drag is given by:

$$\vec{D}_L = \tfrac{1}{2}\rho\left|\vec{V}\right|\vec{V} C_D S \quad (9)$$

where C_D is the drag coefficient of a sphere ($C_D = 0.5$) and S is the sphere cross section.

By enforcing moment equilibrium about the suspension point a system of three second order differential equation in θ_L and φ_L is obtained (here in matrix form):

$$-\vec{R}_L \times \left(-m\vec{a}_L + \vec{F}_G + \vec{D}_L\right) = 0 \quad (10)$$

Any two of these equations is sufficient to compute the solution. The force and the moment applied by the load to the helicopter are:

$$\begin{aligned} \vec{F}_H &= -m\vec{a}_L + \vec{F}_G + \vec{D}_L \\ \vec{M}_H &= \vec{R}_H \times \vec{F}_H \end{aligned} \quad (11)$$

As a remark the differential equations for the pendulum type external load are singular when the cable is aligned to helicopter vertical. This slung load model is in some way limited considering that the elasticity of the cable is neglected. This last point prevents the investigation of the vertical bounce phenomenon particularly significant for light helicopters. This limitations are overcome by the following 6-DOFs rigid body model.

External load as a rigid body

The second approach treats the external load as a rigid body. Nine full non linear equations evaluates linear velocities, angular rates and attitude angles. Three additional equations account for the load centre of mass position in a reference frame. Twelve first order non linear differential equations fully describe the load behaviour. The cable is modelled as elastic but without mass and no aerodynamic effects. A small damping is added.

The six non linear first order differential equations describing rigid body motion are the following:

$$\begin{cases} \dot{u}_L = X_L/m_L + v_L r_L - w_L q_L - g\sin(\theta_L) \\ \dot{v}_L = Y_L/m_L + w_L p_L - u_L r_L + g\sin(\phi_L)\cos(\theta_L) \\ \dot{w}_L = Z_L/m_L + u_L q_L - v_L p_L + g\cos(\phi_L)\cos(\theta_L) \\ \dot{p}_L = L_L/Jx_L - q_L r_L\,(Jz_L - Jy_L)/Jx_L \\ \dot{q}_L = M_L/Jy_L - p_L r_L\,(Jx_L - Jz_L)/Jy_L \\ \dot{r}_L = N_L/Jz_L - p_L q_L\,(Jy_L - Jx_L)/Jz_L \end{cases} \quad (12)$$

The system is derived for the case in which principal moments of inertia of the load are known. Three cinematic equations are added to account for the attitude angles:

$$\begin{cases} \dot{\phi}_L = p_L + q_L\sin(\phi_L)\tan(\theta_L) + r_L\cos(\phi_L)\tan(\theta_L) \\ \dot{\theta}_L = q_L\cos(\phi_L) - r_L\sin(\phi_L) \\ \dot{\psi}_L = q_L\sin(\phi_L)/\cos(\theta_L) + r_L\cos(\phi_L)/\cos(\theta_L) \end{cases} \quad (13)$$

Finally three further equations account for load centre of mass position in an inertial frame. These are, in matrix form:

$$\left[V_{LE}\right] = \left[\dot{x}_{LE}, \dot{y}_{LE}, \dot{z}_{LE}\right]^T = \left[L_{BE_L}\right]\left[u_{LB}, v_{LB}, w_{LB}\right]^T \quad (14)$$

In the previous system of equations, X_L, Y_L, Z_L are the total forces and L_L, M_L, N_L the total moments acting on the load. Defined as vectors:

$$\begin{aligned} \vec{X}_L &= \vec{F}_A + \vec{F}_C \\ \vec{M}_L &= \vec{M}_A + \vec{R}_{LS} \times \vec{F}_C \end{aligned} \quad (15)$$

Where $\vec{F}_A$ and $\vec{F}_C$ are respectively the total aerodynamic forces and the cable forces along each axes, $\vec{M}_A$ are the aerodynamics moments and $\vec{R}_{LS}$ is the position of the suspension point on the load with respect to the load centre of mass defined as:

$$\vec{R}_{LS} = x_{LS}\vec{i}_L + y_{LS}\vec{j}_L + z_{LS}\vec{k}_L \quad (16)$$

The elastic force along the cable F_{Cel} is obtained as follows:

$$\vec{F}_{C_{el}} = -EA\frac{\Delta\vec{L}}{L} \quad (17)$$

where E is the elastic modulus of the material, A is the cross section, L is the nominal length of the cable and $\Delta\vec{L}$ is its elongation. Elongation is obtained by differencing the cable effective length $\vec{L}_{eff}$ and the nominal cable length $\vec{L}$:

$$\Delta\vec{L} = \vec{L}_{eff} - \vec{L} \quad (18)$$

where $\vec{L}_{eff}$ is the difference of the position vector of the suspension point X_{HE} and the position vector of the load centre of mass X_{LE} expressed in an inertial frame:

$$\vec{L}_{eff} = \vec{X}_{HE} - \vec{X}_{LE} \tag{19}$$

The force due to the cable damping is obtained in a similar way:

$$\vec{F}_{C_\zeta} = \zeta \Delta \dot{\vec{L}} \tag{20}$$

where $\Delta\dot{\vec{L}}$ is the difference of the velocity vector of the suspension point $\vec{V}_{HE}$ and the velocity vector of the load centre of mass $\vec{V}_{LE}$ expressed in an inertial frame:

$$\Delta\dot{\vec{L}} = \vec{V}_{HE} - \vec{V}_{LE} \tag{21}$$

and ζ is the damping ratio of the cable defined as:

$$\zeta = 2\frac{\zeta}{\zeta_{crit}}\sqrt{\frac{m_L EA}{L}} \tag{22}$$

where ζ/ζ_{crit} is the ratio of the damping over the critical damping (ζ/ζ_{crit}=0.02) and m_L is the load mass.

A cable applies a force only if stretched. If the instantaneous cable length is below the nominal length the cable doesn't apply any force on the helicopter, thus the total forces and moments applied by the load to the helicopter are:

$$\begin{aligned} \Delta\vec{L} > 0 &\rightarrow \begin{cases} \vec{F}_H = \vec{F}_{Cel} + \vec{F}_{C_\zeta} \\ \vec{M}_H = \vec{R}_H \times \vec{F}_H \end{cases} \\ \Delta\vec{L} \le 0 &\rightarrow \begin{cases} \vec{F}_H = 0 \\ \vec{M}_H = 0 \end{cases} \end{aligned} \tag{23}$$

The great advantage of rigid body formulation is that it allows to take into account aerodynamic effects and inertial properties of the load. The main disadvantage is the increased dimension of the system of differential equations needed to describe the system.

Spherical load

For comparison purposes the first load studied is modelled as a sphere. As in the previous case only isotropic drag applies to the load. Inertial properties of the body are:

$$J_{X_L} = J_{Y_L} = J_{Z_L} = \frac{2}{5} m_L r_L^2 \tag{24}$$

where r_L is the radius of the sphere. As in the previous case aerodynamic forces and moments reduce to:

$$\begin{aligned} \vec{F}_A &= \vec{D}_L = \tfrac{1}{2}\rho\left|\vec{V}\right|\vec{V}C_D S \\ \vec{M}_A &= 0 \end{aligned} \tag{25}$$

Finned body

The second type of load studied is a streamlined finned body with cruciform tail surfaces. To determine inertial properties the body is considered an ellipsoid with principal semi-axes with the following properties:

$$b = c < a \qquad \begin{aligned} r_L &= b = c \\ l_L &= a \end{aligned} \tag{26}$$

where *a, b, c* are respectively the principal semi-axes along *x, y, z*. Hence, considering uniform density, the inertial properties of the body are:

$$\begin{aligned} J_x &= \frac{2}{5} m_L r_L^2 \\ J_y &= J_z = \frac{1}{5} m_L \left(l_L^2 + r_L^2\right) \end{aligned} \tag{27}$$

where r_L, l_L and m_L are respectively the maximum radius, the length and the mass of the body.

Aerodynamic forces acting on the body are:

$$\begin{aligned} D_L &= \frac{1}{2}\rho V^2 S C_D & C_D &= C_{D_0} + k\left(C_L^2 + C_S^2\right) \\ L_L &= \frac{1}{2}\rho V^2 S C_L & C_L &= C_{L\alpha}\alpha \\ S_L &= \frac{1}{2}\rho V^2 S C_S & C_S &= C_{L\alpha}\beta \end{aligned} \tag{28}$$

where due α is the angle of attack, β is the angle of sideslip and $S = \pi r_L^2$ is the body cross section. Aerodynamic symmetry is assumed.

Aerodynamic moments are:

$$\begin{aligned} M_L &= \frac{1}{2}\rho V^2 S C_M & C_M &= C_L x_A \\ N_L &= \frac{1}{2}\rho V^2 S C_N & C_N &= C_S x_A \end{aligned} \tag{29}$$

where x_A is the distance between the centre of mass of the body and its aerodynamic centre. Due to the axial symmetry no rolling moment is considered.

Stability Augmentation System (SAS)

Helicopters usually show a mildly unstable response, thus, SAS is often fitted to enhance stability and controllability. Two different implementations are applied to the present model in order to investigate their performance during the release phase of an external load (drop test).

SAS 1

The first system considered is a conventional SAS in which the longitudinal attitude angle θ and the relative angular rate q are used as a feedback to the longitudinal cyclic, while the roll angle φ and the roll angular rate p for the lateral cyclic. The controls are:

$$\begin{aligned} \delta_{lon} &= K_\theta(\theta - \theta_{ref}) + K_q q \\ \delta_{lat} &= K_\phi(\phi - \phi_{ref}) + K_p p \end{aligned} \tag{30}$$

SAS 2

The second SAS is similar to the first one but a further loop is closed by feeding back the variation of the vertical force (load cell measurement at the suspension point) to the collective pitch. Changing the collective pitch leads to a change in the torque applied by the rotor to the fuselage, with a consequent yawing motion. To avoid that, mixing with the pedal input is provided. The complete control vector is:

$$\begin{aligned} \delta_0 &= K_w(w-w_{ref})+K_{\dot{w}}\dot{w} \\ \delta_{lon} &= K_\theta(\theta-\theta_{ref})+K_q q \\ \delta_{lat} &= K_\phi(\phi-\phi_{ref})+K_p p \\ \delta_{ped} &= \delta_0 \end{aligned} \quad (31)$$

where:

$$\begin{aligned} w &= \int_0^t \frac{\Delta Z_H}{m_H} \\ \dot{w} &= \frac{\Delta Z_H}{m_H} \end{aligned} \quad (32)$$

where w is the climb rate induced by the release of the external load, $\dot{w}$ is the vertical acceleration and Z_H is the vertical force applied by the load to the suspension point.

Solution Technique

To account for load effects, helicopter equations have to be modified. In particular the differences between the equilibrium forces and moments and the actual forces and moments applied to the helicopter by the suspended load must be added to the vehicle dynamics. The first six helicopter equation are modified as follows:

$$\begin{cases} \dot{u} = \dfrac{\Delta X_H}{m_H}+\sum\limits_{i=1}^{9} A_{1,i}x_i \\ \dot{v} = \dfrac{\Delta Y_H}{m_H}+\sum\limits_{i=1}^{9} A_{2,i}x_i \\ \dot{w} = \dfrac{\Delta Z_H}{m_H}+\sum\limits_{i=1}^{9} A_{3,i}x_i \end{cases} \quad \begin{cases} \dot{p} = L'_H+\sum\limits_{i=1}^{9} A_{4,i}x_i \\ \dot{q} = \Delta M_H+\sum\limits_{i=1}^{9} A_{5,i}x_i \\ \dot{r} = N'_H+\sum\limits_{i=1}^{9} A_{6,i}x_i \end{cases} \quad (33)$$

where:

$$L'_H = \frac{\Delta L_H + \dfrac{J_{xz_H}}{J_{x_H}}\Delta N_H}{1-\dfrac{J^2_{xz_H}}{J_{x_H}J_{z_H}}} \quad N'_H = \frac{\Delta N_H + \dfrac{J_{xz_H}}{J_{z_H}}\Delta L_H}{1-\dfrac{J^2_{xz_H}}{J_{x_H}J_{z_H}}} \quad (34)$$

Where ΔL_H, ΔM_H and ΔN_H are already normalised with their respective moments of inertia J_{x_H}, J_{y_H} and J_{z_H}. It is now possible to linearise the full system of differential equations composed by 9+3 helicopter equations and, depending on the chosen model, the 4/9+3 suspended load equations. Linearization is performed through the residues method. Starting from a trimmed condition, the states, the controls and the derivative vector are iteratively perturbed. It is then possible to reconstruct a linear system of differential equations in the following form:

$$[E]\{d\dot{x}\}+[A_1]\{dx\}+[B_1]\{du\}=0 \quad (35)$$

where [E], [A_1] and [B_1] matrices are built as follows:

$$[A_1]=\begin{bmatrix} \dfrac{f_{11}-f_{01}}{\Delta x} & \cdots & \dfrac{f_{n1}-f_{01}}{\Delta x} \\ \vdots & \ddots & \vdots \\ \dfrac{f_{1n}-f_{0n}}{\Delta x} & \cdots & \dfrac{f_{nn}-f_{0n}}{\Delta x} \end{bmatrix} \quad (36)$$

where:

$$f = f(\dot{x},x,u) \quad (37)$$

is the residual of the single differential equation. The impact of the increment Δx in the range $10^{-4} \div 10^{-1}$ was found to be negligible in present model formulation. Hence, it is possible to derive a state space system:

$$\begin{aligned} \{d\dot{x}\} &= -[E]^{-1}[A_1]\{dx\}-[E]^{-1}[B_1]\{du\} \\ \{d\dot{x}\} &= [A]\{dx\}+[B]\{du\} \end{aligned} \quad (38)$$

The resulting formulation is used to assess the dynamic stability of the system by modal response analysis.

The non linearised equations are used to evaluate short term time response. In particular helicopter dynamics after impulsive load separation is assessed.

Results

The nominal characteristics for the reference helicopters are given in Tab. 2. For the present analysis $\vec{R}_H = \vec{R}_{LS} = 0$.

	Helicopter 1	**Helicopter 2**
$m_{TOT} = m_H + m_L$ [kg]	6791	15876
m_L [kg]	1360	3175
m_L/m_{TOT} [%]	20	20
L [m]	5	5
C_{DS} [m^2]	0.5	0.5

Tab. 2 – Helicopter reference conditions

Two types of analysis are performed: I) a preliminary assessment of dynamic stability of the coupled system in forward flight and II) an example of time domain response to perturbation for different levels of stability augmentation. All the stability plots (real and imaginary parts of the eigenvalues) assume that the total weight m_{TOT} is constant i.e. the weight of the slung load is subtracted to the bare airframe nominal weight (with the exception of Fig. 8). The stability matrix [A] and the control matrix [B] are multiplied by a scaling factor $m_{TOT}/(m_{TOT}-m_L)$ in order to correct the sensitivity of the system as a consequence of helicopter mass reduction. The plots include the boundaries for pitch and roll oscillations as addressed by Ref. [18]. These requirements apply only to the helicopter poles, and not to the load poles.

The effect of slung load model on stability plots is presented in Figs. 2÷4 for Helicopter 1 and Figs. 5÷7 for Helicopter 2.

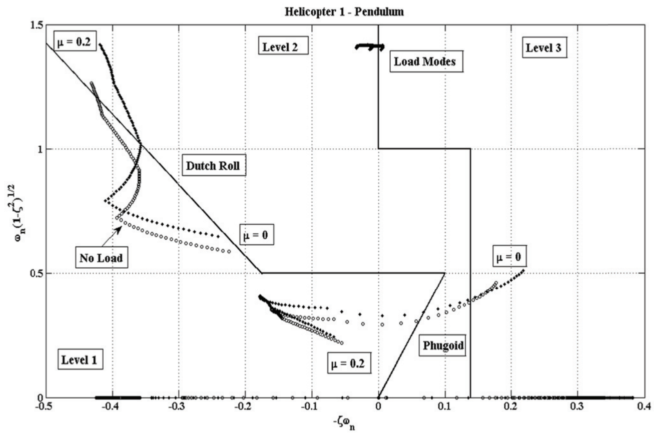

Fig. 2 – Helicopter 1, pendulum model, $m_{TOT} = m_L + m_H = 6791$ kg, $m_L = 0$; 1360 kg, L = 5 m, $C_DS = 0.5$ m^2, μ = 0 ÷ 0.2

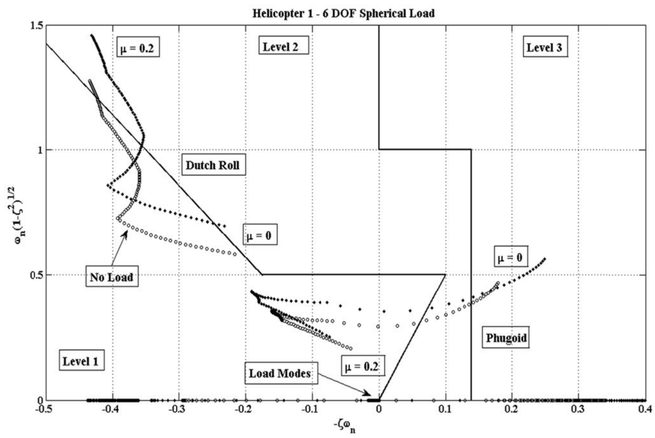

Fig. 3 – Helicopter 1, 6 DOF model, spherical load, $m_{TOT} = 6791$ kg, $m_L = 0$; 1360 kg, L = 5 m, $C_DS = 0.5$ m^2, μ = 0 ÷ 0.2

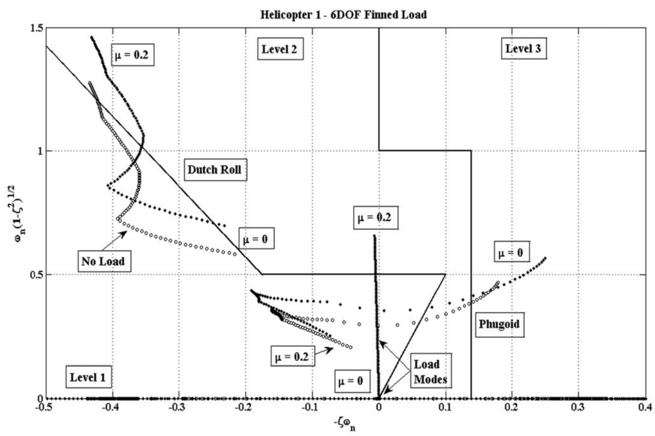

Fig. 4 – Helicopter 1, 6 DOF model, finned load, $m_{TOT} = 6791$ kg, $m_L = 0$; 1360 kg, L = 5 m, $C_DS = 0.5$ m^2, μ = 0 ÷ 0.2

The poles of the coupled system are plotted for the pendulum type model in Fig. 2. The oscillatory modes of the vehicle (phugoid and Dutch roll) exhibit a marginal effect of the suspended load, which is characterized by a lightly damped separate oscillatory response (as shown in Ref. [11]) with its natural frequency matching the classical pendulum equation $\omega_n = \sqrt{g/L}$. The lateral-directional oscillatory mode (Dutch roll) degrades its stability for higher advance ratios when the load is present. The results for the equivalent spherical load obtained with the 6 DOFs rigid body model (see Fig. 3) reproduce very similar trends for phugoid and Dutch roll, while the load is characterized by lightly damped non oscillatory modes (real eigenvalues). Note that these last results include cable elasticity. The aerodynamics of the load is still modelled as a drag vector (as in Fig. 2). In Fig. 4, the load is replaced by an ellipsoid with equivalent mass properties, stabilized by cruciform tail-planes. The present analysis is performed assuming linear aerodynamics, while in the real case the suspended system is usually characterized by separation and wake patterns that may induce non linearities and changes in the dynamic stability of the slung load. No aerodynamic damping is considered. The oscillatory response of the vehicle matches the previous cases, confirming that the coupling mechanism is mainly driven by the force transmission from the load to the helicopter (vector aligned with the cable). The load is characterized by an oscillatory short period mode (eigenvector: w_L, q_L, θ_L) with marginal dynamic stability - as the aerodynamic damping is still neglected - and real modes mainly affecting lateral-directional response (dihedral effect is missing i.e. destabilizing the spiral mode of the suspended load). In all three cases, the vehicle also shows a degradation of its stability with increasing forward speed (eigenvector: u_H, θ_H) further destabilized by the presence of the suspended load.

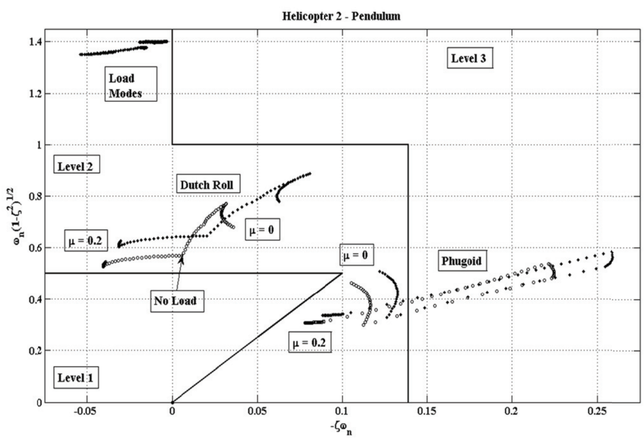

Fig. 5 – Helicopter 2, pendulum model, $m_{TOT} = 15876$ kg, $m_L = 0$; 3175 kg, L = 5 m, $C_DS = 0.5$ m^2, μ = 0 ÷ 0.2

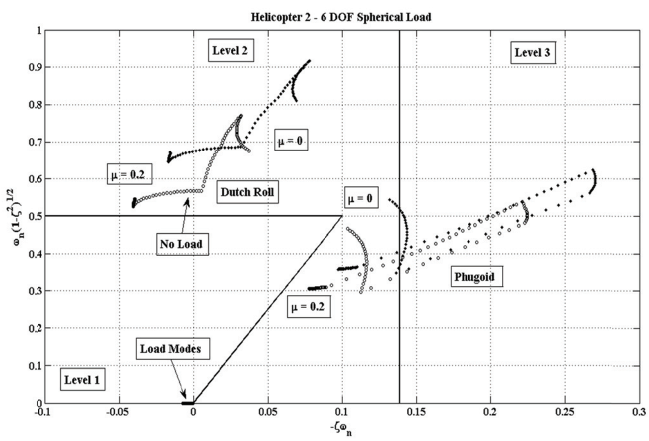

Fig. 6 – Helicopter 2, 6 DOF model, spherical load, $m_{TOT} = 15876$ kg, $m_L = 0$; 3175 kg, L = 5 m, $C_DS = 0.5$ m^2, μ = 0 ÷ 0.2

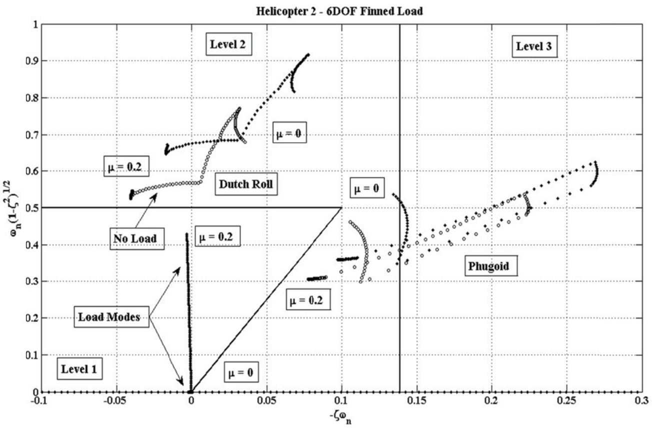

Fig. 7 – Helicopter 2, 6 DOF model, finned load, m_{TOT} = 15876 kg, m_L = 0; 3175 kg, L = 5 m, C_DS = 0.5 m^2, μ = 0 ÷ 0.2

The results for Helicopter 2 differ as the trend for phugoid and Dutch roll shows lower levels of dynamic stability and different behaviours for increasing advance ratios. The other modal responses of the bare airframe are stable, differently from Helicopter 1. As a remark, the data for Helicopter 2 derive from parametric models based on flight tests (see Ref. [21]) interpolated for intermediate forward speeds. The results confirm that the model for the suspended load and its level of complexity only affect the rigid body response of the load while the moderate coupling with the helicopter dynamic behaviour is substantially unchanged.

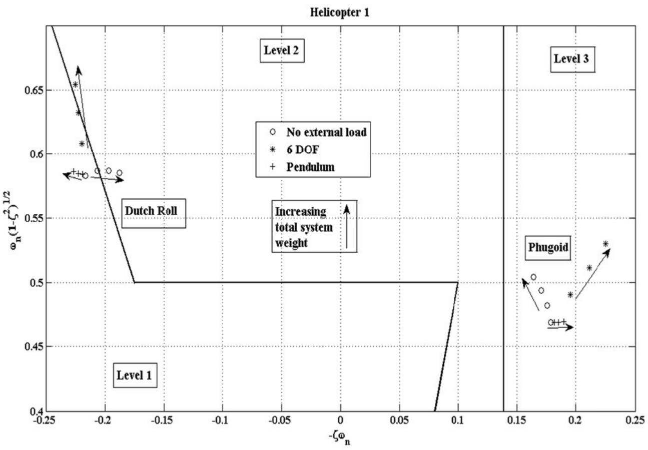

Fig. 8 – Helicopter 1, bare airframe, pendulum and 6 DOF spherical load models, m_{TOT} = 6791; 7470; 8149; 8828 kg, m_L = 0; 680; 1360; 2040 kg, L = 5 m, C_DS = 0.5 m^2, μ = 0

The effect of total mass m_{TOT} on phugoid and Dutch roll in hover is outlined in Fig. 8, in which the poles are compared for either onboard or external weight increase. The trend of eigenvalues for increasing bare airframe mass differs from the external load cases for both pendulum and 6DOFs type model. The data for the bare airframe derive from dynamic condensation of the higher order model for Helicopter 1 used in Ref. [11]. The 6DOFs type model predicts a stability degradation in hover differently from the pendulum type model. Quite probably, the bouncing of the suspended mass in hover alters in a more evident way the oscillatory behaviour of the helicopter. This is enhanced by the elasticity of the cable, neglected for the pendulum type model.

Some relevant parametric effects were investigated (mass m_L, cable length L, drag area C_DS and cable damping) for spherical type suspended load, comparing the stability of the system for both pendulum and 6DOFs type models.

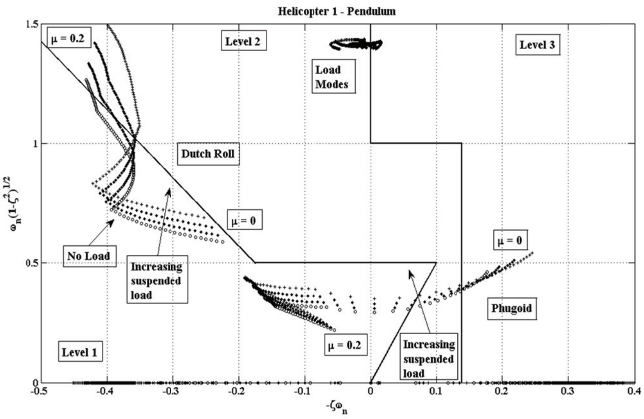

Fig. 9 – Helicopter 1, pendulum model, m_{TOT} = 6791 kg, m_L = 0; 680; 1360; 2040 kg, L = 5 m, C_DS = 0.5 m^2, μ = 0 ÷ 0.2

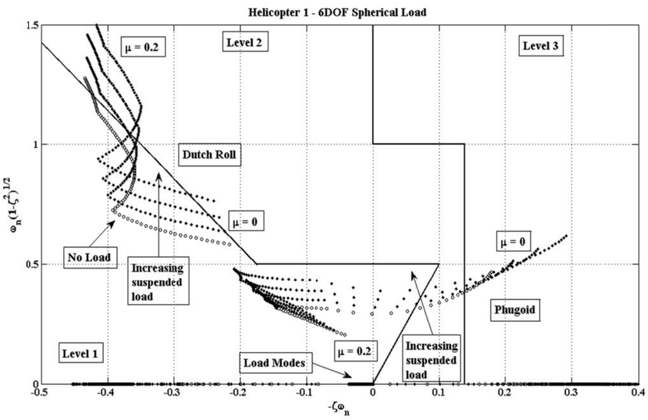

Fig. 10 – Helicopter 1, 6 DOF model, spherical load, m_{TOT} = 6791 kg, m_L = 0; 680; 1360; 2040 kg, L = 5 m, C_DS = 0.5 m^2, μ = 0 ÷ 0.2

In Figs. 9÷10 the effect of suspended mass m_L is considered. The level of coupling with the oscillatory modes of the helicopter (phugoid and Dutch roll) is larger for heavier suspended masses. Large slung loads also induce a degradation of stability on lateral-directional response for higher advance ratios, while low frequency longitudinal dynamics seems to be quite insensitive to their effects. The impact of modelling of the suspended load is not evident.

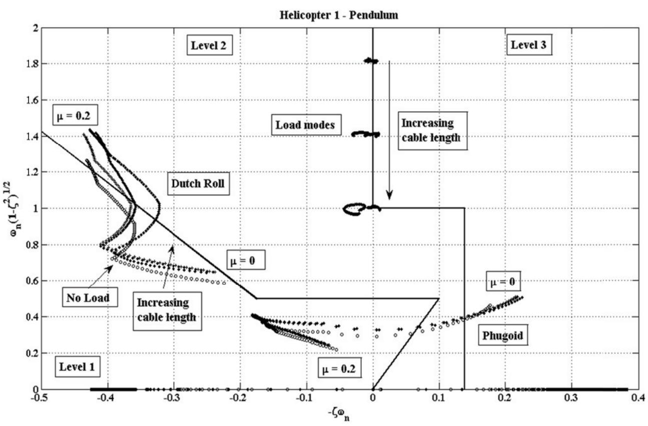

Fig. 11 – Helicopter 1, pendulum model, m_{TOT} = 6791 kg, m_L = 0; 1360kg, L = 3; 5; 10 m, C_DS = 0.5 m^2, μ = 0 ÷ 0.2

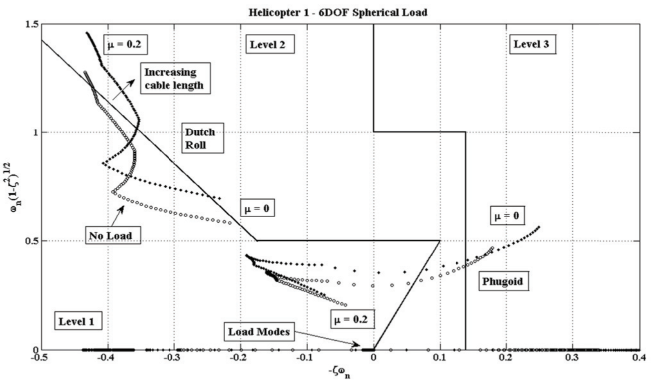

Fig. 12 – Helicopter 1, 6 DOF model, spherical load, m_{TOT} = 6791 kg, m_L = 0; 1360kg, L = 3; 5; 10 m, C_DS = 0.5 m^2, μ = 0 ÷ 0.2

In Figs. 11÷12 the effect of cable length L is presented. The pendulum reacts as expected changing the natural frequency of the oscillatory modes of the load. As in other parametric effects, the most evident consequence of changing the length of the pendulum is the higher level of coupling with lateral-directional modes, mainly visible for higher forward speeds and shorter cables. Differently, when the same analysis is performed with the 6DOFs model with the elastic suspension (Fig. 12), the response is quite unaffected by the change of cable length (i.e. by the change of the stiffness of the cable as the section is unchanged). Note that, for the pendulum type model the attitude of the payload is enforced by the angular displacement of the cable. Hence, this last result derives from the independent attitude dynamics of the payload for the 6DOFs model, probably providing a more realistic representation of the suspended load.

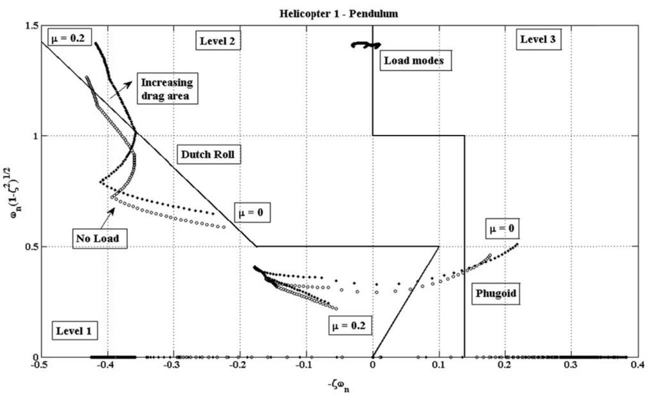

Fig. 13 – Helicopter 1, pendulum model, m_{TOT} = 6791 kg, m_L = 0; 1360kg, L = 5 m, C_DS = 0.5; 1; 2 m^2, μ = 0 ÷ 0.2

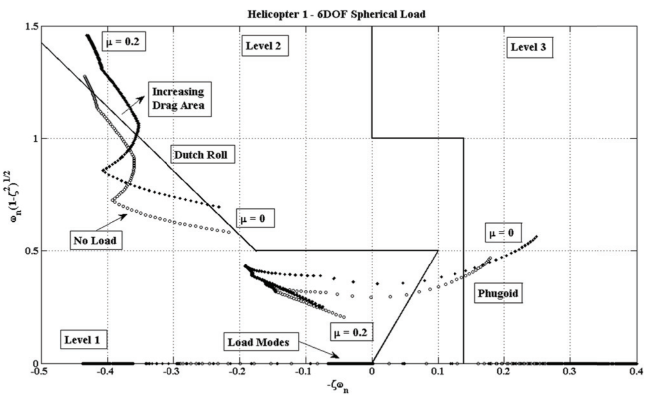

Fig. 14 – Helicopter 1, 6 DOF model, spherical load, m_{TOT} = 6791 kg, m_L = 0; 1360kg, L = 5 m, C_DS = 0.5; 1; 2 m^2, μ = 0 ÷ 0.2

In Figs. 13÷14 the role of drag area C_DS is outlined. This effect is apparently hardly observable as, within the limits of the present parametric changes (C_DS = 0.5 ÷ 2 m^2), the eigenvalues for both the vehicle and the load respond very mildly to the drag increment. The only relevant effect is the stabilization of the load modes (real eigenvalues) for the 6DOFs model (Fig. 14).

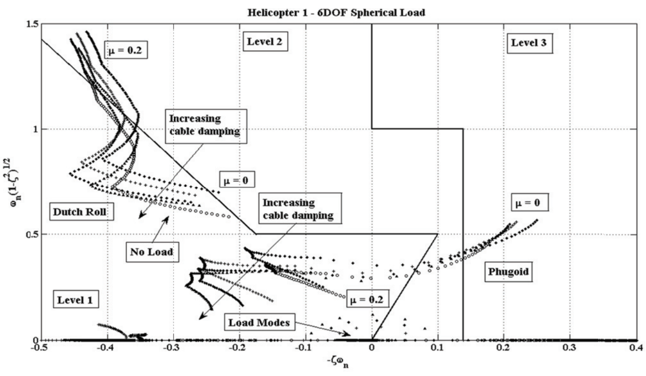

Fig. 15 – Helicopter 1, 6 DOF model, spherical load, m_{TOT} = 6791 kg, m_L = 0; 1360kg, L = 5 m, C_DS = 0.5 m^2, ζ/ζ_{crit} = 0; 0.01; 0.02; 0.03, μ = 0 ÷ 0.2

The effect of cable damping is plotted in Fig. 15. The damping ratio of the suspension system (neglected in all previous results presented for the 6DOFs suspended load model) does actually stabilize the oscillatory modes of the helicopter (both phugoid and Dutch roll modes). This point suggests that modelling the cable as a rigid suspension or neglecting its elongation rate may preclude the completeness of the stability analysis of helicopter suspended loads.

The 6DOFs model for the suspended load was also used to reproduce the time-domain response of Helicopter 1 during the release phase of the suspended load. This simulation is performed for μ = 0.1 as a starting condition for the reference configuration presented in Tab. 2. A fixed time step integrator has been used (Δt = 10^{-2} s). Two different levels of stability augmentation of the airframe are compared with the natural response of the helicopter. The details on the stability augmentation system implementation are given in the previous sections.

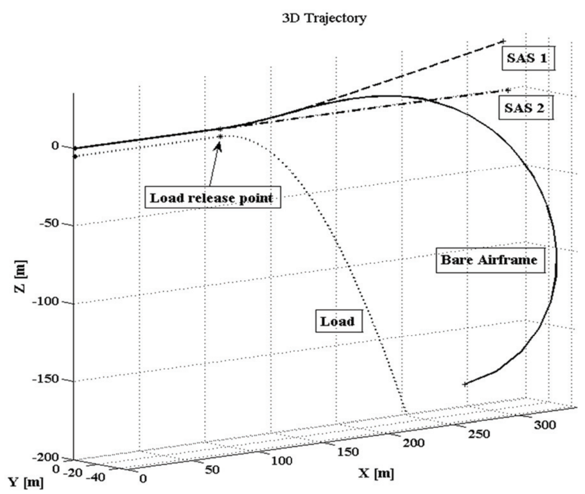

Fig. 16 – Load release (3D trajectory): no SAS, SAS 1, SAS 2. Helicopter 1, 6 DOF model, finned load, , m_{TOT} = 6791 kg, m_L = 0; 1360kg, L = 5 m, C_DS = 0.5 m^2, μ = 0.1

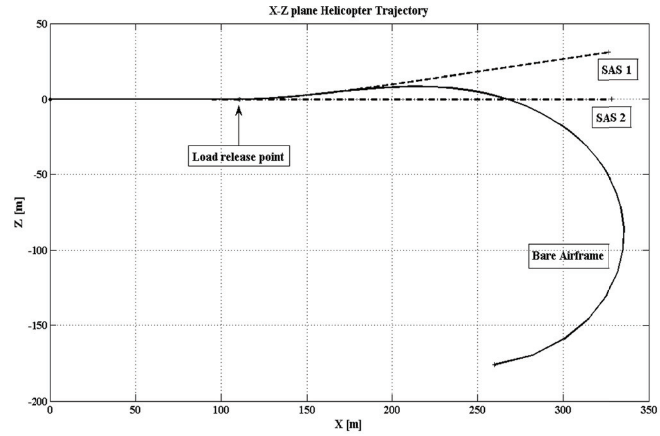

Fig. 17 – Load release (X-Z plane trajectory): no SAS, SAS 1, SAS 2. Helicopter 1, 6 DOF model, finned load, m_{TOT} = 6791 kg, m_L = 0; 1360kg, L = 5 m, C_DS = 0.5 m^2, μ = 0.1

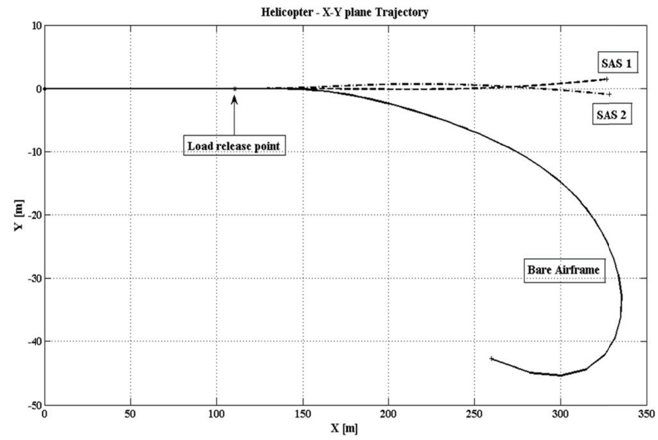

Fig. 18 – Load release (X-Y plane trajectory): no SAS, SAS 1, SAS 2. Helicopter 1, 6 DOF model, finned load, m_{TOT} = 6791 kg, m_L = 0; 1360kg, L = 5 m, C_DS = 0.5 m^2, μ = 0.1

The short-term response of the bare airframe is found to diverge from equilibrium as soon as the load is dropped (see Figs. 16÷18). Attitude stabilization (SAS1) does compensate the tendency to abandon the initial trajectory induced by the impulsive mass change but still the altitude response drifts from the initial level flight, as expected due to untrimmed collective. When collective feedback is super-imposed to attitude stabilization (SAS2), the vehicle follows closely the initial flight parameters.

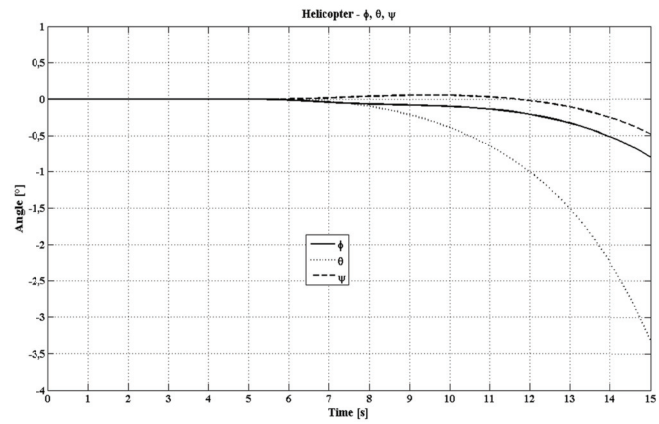

Fig. 19 – Load release (Helicopter Euler angles): no SAS. Helicopter 1, 6 DOF model, finned load, m_{TOT} = 6791 kg, m_L = 0; 1360kg, L = 5 m, C_DS = 0.5 m^2, μ = 0.1

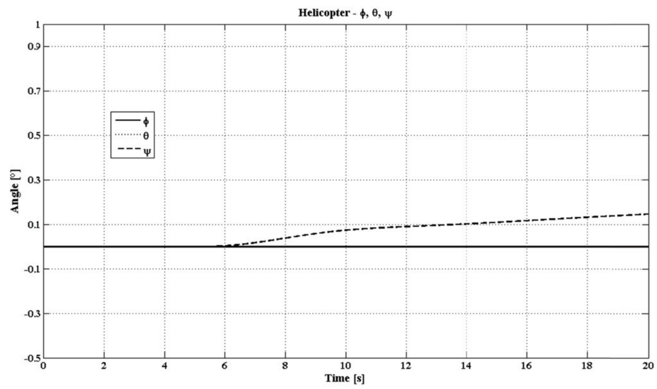

Fig. 20 – Load release (Helicopter Euler angles): SAS 1. Helicopter 1, 6 DOF model, finned load, m_{TOT} = 6791 kg, m_L = 0; 1360kg, L = 5 m, C_DS = 0.5 m^2, μ = 0.1

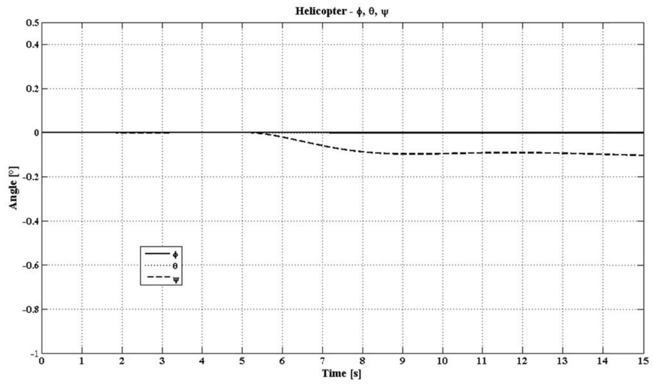

Fig. 21 – Load release (Helicopter Euler angles): SAS 2. Helicopter 1, 6 DOF model, finned load, m_{TOT} = 6791 kg, m_L = 0; 1360kg, L = 5 m, C_DS = 0.5 m^2, μ = 0.1

The attitude response of the helicopter after the load release is presented in Figs. 19÷21, and it confirms that the level of stability augmentation is substantially beneficial in terms of stability of the trajectory. These simulations do not imply any general conclusion on the validity of the augmentation strategy proposed, as no comparison with reference flight test data is available for validation purposes. Nevertheless, this time domain analysis confirms the availability of a light simulation model of helicopter and slung load system, in which the fidelity of the simulation is preserved for the bare airframe and the level of complexity of model for the suspended load is sufficiently extended. This type of intermediate models may be helpful in the preliminary assessment of stability and control augmentation systems, requiring a very limited computational workload.

CONCLUDING REMARKS

In the present work a simple state space helicopter model is coupled with a pendulum and then with a 6DOFs suspended external load model. The system stability is evaluated changing the type of helicopter, the type of slung load model and the load parameters. The impact of advance ratio is superimposed in the different cases.

Modal analysis outlines that the slung load model is coupled with the oscillatory dynamics of the helicopter through the force applied by the cable in the suspension point. The attitude dynamics of the suspended load has a minor role in the coupling of the two subsystems. Comparisons for different mass increases show that a direct increase of helicopter fuselage weight is not equivalent to suspending an additional mass underneath the vehicle.

Cable damping is apparently providing a source of additional dynamic stability to the coupled system. The comparison, between the pendulum type model and the 6DOFs type model for the slung load, points out the limitations of the first approach, in some way over simplifying the natural dynamics of the suspended rigid body.

Short term time domain responses, with different levels of helicopter stability augmentation, show that the proposed model, at least in its most complete formulation, is adequate to represent the impact of control design parameters on the response of the system. As a final comment, it is demonstrated that the 6DOFs type model for the suspended load may account for inertial and aerodynamics complexity of the slung load with very limited computational workload.

Reported pilot experience validates, at least partially, the results obtained. In fact aerodynamic effects and cable length are known to have little effect on the dynamic behaviour of helicopter with suspended loads similar to those here considered (heavy weight, small C_DS). On the contrary helicopter dynamics in case of low density loads is much more influenced by aerodynamics and cable length. In particular short cables expose the load to the main rotor downwash. The implementation of the main rotor downwash in the present model would help to extend its validity to a wider range of external suspended loads. In any case validation with flight test data would be advisable for future developments of this research activity.

ACKNOWLEDGMENT

This activity is part of a doctoral research program (Ph.D. in Aerospace Engineering at Politecnico di Torino) supported by AgustaWestland for which Riccardo Bianco Mengotti and Andrea Ragazzi are the industrial supervisors.

REFERENCES

[1] Manwaring J. C., Conway G. A., and Garrett L. C., "Epidemiology and Prevention of Helicopter External Load Accidents", *Journal of Safety Research*, Vol. 29, No. 2, pp. 107–121, 1998

[2] Lucassen, L. R. and Sterk, F. J., "Dynamic Stability Analysis of a Hovering Helicopter With a Sling Load", *Journal of American Helicopter Society*, Vol. 10, pp. 6-12, April 1965

[3] Szustack L.S., Jenney D., "Control of Large Crane Helicopters", *Journal of American Helicopter Society*, Vol.16, No. 3, pp. 11-22, July 1971

[4] Dukes, T.A., "Manoeuvring Heavy Sling load Near Hover, Part I: Damping the Pendulous Motion", *Journal of American Helicopter Society*, Vol. 18, No. 2, pp. 2-11, April 1973

[5] Dukes, T.A., "Manoeuvring Heavy Sling load Near Hover, Part I: Some Elementary Manoeuvres", *Journal of American Helicopter Society*, Vol. 18, No. 3, pp. 17-22, July 1973

[6] Thanapalan K., Wong T. M. "Modelling of a Helicopter with an Under-Slung Load System" *Proceedings of the 29th Chinese Control Conference*, Beijing, China, July 29-31, 2010

[7] Nagabhushan B,. L., "Low-Speed Stability Characteristics of a Helicopter With a Sling Load", *Vertica*, Vol. 9, 1985

[8] Poli C. and Cormack D., "Dynamics of Slung Bodies Using a Single Point Suspension System", *Journal of Aircraft*, Vol. 12, No.10, pp. 773-777, October 1975

[9] Cliff E. M. and Bailey D. B., "Dynamic Stability of a Translating Vehicle with a Simple Sling Load", *Journal of Aircraft*, Vol. 12, No.10, pp. 849-856, October 1975

[10] Cicolani L. S., McCoy, A. H., Tischlel, M. B., Tucker, G. E., Gatenio, P., and Marmar, D., "Flight-Time Identification of a UH-60A Helicopter and Slung Load", *Proceedings of the NATO RTA Symposium on System Identification for Integrated Aircraft Development and Flight Testing*, Madrid, Spain, May 1998

[11] Fusato D., Guglieri G., Celi R., "Flight Dynamics of an Articulated Rotor Helicopter with an External Slung Load", *American Helicopter Society*, Vol. 46, pp. 3-13, 2001

[12] Guglieri G., Quagliotti F., "Effect of Main Rotor Configuration and Propulsion System Dynamics on Helicopter Handling Qualities ", *21st ICAS Congress, Conference Proceedings,* Melbourne, Australia, September 1998.

[13] Cicolani L., Cone A., Theron J. N., Robinson D., Lusardi J., Tischler M. B., Rosen A., Raz R., "Flight Test and Simulation of a Cargo Container Slung Load in Forward Flight", *Journal of American Helicopter Society*, Vol. 54, 2010

[14] L. S. Cicolani, J. G. A. da Silva, E. P. N. Duque, M. B. Tischler "Unsteady aerodynamic model of a cargo container for slung-load simulation", *The Aeronautical Journal*, Vol. 108, pp. 357-368, July 2004

[15] Raz R., Rosen A., Carmeli A., Lusardi J., Cicolani, L. Robinson D., "Wind Tunnel and Flight Evaluation of Passive Stabilization of a Cargo Slung Load", *Journal of American Helicopter Society*, Vol. 55, No. 3, 2010

[16] Cicolani, L. S., Kanning, G., "Equations of Motion of Slung-Load Systems, Including Multilift Systems", *NASA TP 3280*, Nov. 1992

[17] Bisgaard M., Bendtsen J. D., la Cour-Harbo A. "Modelling of Generic Slung Load System", *Proceedings of the AIAA Modelling and Simulation Technologies*, 2006

[18] Anonymous, ADS-33E-PRF, "Aeronautical Design Standard, Performance Specification, Handling Qualities Requirements for Military Rotorcraft",

United States Army Aviation and Missile Command, Aviation Engineering Directorate, Redstone Arsenal, Alabama, March 21, 2000

[19] Roger H. Hoh, Robert K. Heffley, David G. Mitchell "Development of Handling Qualities Criteria for Rotorcraft with Externally Slung Loads", *NASA/CR–2006–213488*, October 2006

[20] Padfield, G.D., "On the Use of Approximate Models in Helicopter Flight Mechanics", *Vertica*, Vol. 5, pp. 243-259, 1981

[21] Heffley R.K., Jewell W.F., Lehman J.M., Van Winkle R.A., "A Compilation and Analysis of Helicopter Handling Qualities Data – Volume One: Data Compilation", *NASA Contractor Report 3144*, 1975